

All-solid highly nonlinear singlemode fibers with a tailored dispersion profile

Francesco Poletti,* Xian Feng, Giorgio M. Ponzo, Marco N. Petrovich, Wei H. Loh, David J. Richardson

Optoelectronics Research Centre, University of Southampton, Southampton, SO17 1BJ, UK
*frap@orc.soton.ac.uk

Abstract: We investigate a novel approach to obtain highly nonlinear fibers with a tailored group velocity dispersion around a desired wavelength region of interest. Rather than exploiting longitudinal holes to control the average refractive index of the cladding and hence the fiber's waveguide dispersion, as in holey fibers, we propose using an all-solid cladding with a suitably chosen refractive index difference relative to the core. We demonstrate numerically that this solution allows a large freedom in the manipulation of the overall fiber dispersive properties, while enabling, in practice, a much more accurate control of the fiber's structural properties during fabrication. Effectively single mode guidance over a broad wavelength range can be achieved through the use of a second outer cladding forming a W-type index profile. We derive simple design rules for dispersion controlled fibers, based on which an algorithm for the automatic dispersion optimization is proposed, implemented and used to design various nonlinear fibers for all-optical processing and supercontinuum generation. Fabrication of a lead silicate fiber with flattened dispersion at telecoms wavelengths confirms the potential of these new fibers.

©2010 Optical Society of America

OCIS codes: (060.2280) Fiber design and fabrication; (060.4370) Nonlinear optics, fibers.

References and links

1. G. P. Agrawal, *Nonlinear fiber optics*, 3rd ed. (Academic Press, San Diego, 2001).
2. J. P. Gordon, "Theory of the soliton self-frequency shift," *Opt. Lett.* **11**(10), 662–664 (1986).
3. A. V. Gorbach, and D. V. Skryabin, "Light trapping in gravity-like potentials and expansion of supercontinuum spectra in photonic-crystal fibres," *Nat. Photonics* **1**(11), 653–657 (2007).
4. F. Poletti, P. Horak, and D. J. Richardson, "Soliton spectral tunneling in dispersion-controlled holey fibers," *IEEE Photon. Technol. Lett.* **20**(16), 1414–1416 (2008).
5. J. M. Dudley, G. Genty, and S. Coen, "Supercontinuum generation in photonic crystal fiber," *Rev. Mod. Phys.* **78**(4), 1135–1184 (2006).
6. J. M. Stone, and J. C. Knight, "Visibly "white" light generation in uniform photonic crystal fiber using a microchip laser," *Opt. Express* **16**(4), 2670–2675 (2008).
7. J. H. V. Price, T. M. Monro, H. Ebendorff-Heidepriem, F. Poletti, P. Horak, V. Finazzi, J. Y. Y. Leong, P. Petropoulos, J. C. Flanagan, G. Brambilla, M. Feng, and D. J. Richardson, "Mid-IR supercontinuum generation from nonsilica microstructured optical fibers," *IEEE J. Sel. Top. Quantum Electron.* **13**(3), 738–749 (2007).
8. M. Takahashi, R. Sugizaki, J. Hiroishi, M. Tadakuma, Y. Taniguchi, and T. Yagi, "Low-loss and low-dispersion-slope highly nonlinear fibers," *J. Lightwave Technol.* **23**(11), 3615–3624 (2005).
9. J. C. Knight, T. A. Birks, P. S. Russell, and D. M. Atkin, "All-silica single-mode optical fiber with photonic crystal cladding," *Opt. Lett.* **21**(19), 1547–1549 (1996).
10. J. C. Knight, J. Arriaga, T. A. Birks, A. Ortigosa-Blanch, W. J. Wadsworth, and P. S. Russell, "Anomalous dispersion in photonic crystal fiber," *IEEE Photon. Technol. Lett.* **12**(7), 807–809 (2000).
11. M. L. V. Tse, P. Horak, F. Poletti, N. G. R. Broderick, J. H. V. Price, J. R. Hayes, and D. J. Richardson, "Supercontinuum generation at 1.06 μm in holey fibers with dispersion flattened profiles," *Opt. Express* **14**(10), 4445–4451 (2006).
12. W. H. Reeves, J. C. Knight, P. S. J. Russell, and P. J. Roberts, "Demonstration of ultra-flattened dispersion in photonic crystal fibers," *Opt. Express* **10**(14), 609–613 (2002).
13. K. Hansen, "Dispersion flattened hybrid-core nonlinear photonic crystal fiber," *Opt. Express* **11**(13), 1503–1509 (2003).
14. K. Saitoh, M. Koshiba, T. Hasegawa, and E. Sasaoka, "Chromatic dispersion control in photonic crystal fibers: application to ultra-flattened dispersion," *Opt. Express* **11**(8), 843–852 (2003).

15. F. Poletti, V. Finazzi, T. M. Monro, N. G. R. Broderick, V. Tse, and D. J. Richardson, "Inverse design and fabrication tolerances of ultra-flattened dispersion holey fibers," *Opt. Express* **13**(10), 3728–3736 (2005).
16. X. Feng, F. Poletti, A. Camerlingo, F. Parmigiani, P. Petropoulos, P. Horak, G. M. Ponzio, M. N. Petrovich, W. H. Loh, and D. J. Richardson, "Dispersion controlled highly nonlinear fibers for all optical processing at telecoms wavelengths," *Opt Fiber Technol* (invited and submitted, 2010).
17. A. W. Snyder, and X. H. Zheng, "Optical Fibers of Arbitrary Cross-Sections," *J. Opt. Soc. Am. A* **3**(5), 600–609 (1986).
18. A. W. Snyder, and J. D. Love, *Optical waveguide theory* (Chapman and Hall, London; New York, 1983).
19. A. Ferrando, E. Silvestre, P. Andres, J. Miret, and M. Andres, "Designing the properties of dispersion-flattened photonic crystal fibers," *Opt. Express* **9**(13), 687–697 (2001).
20. Schott Optical glass catalogue 2009, available from <http://www.schott.com>.
21. J. A. Nelder, and R. Mead, "A simplex method for function minimization," *Comput. J.* **7**, 308–313 (1965).
22. T. M. Monro, and H. Ebendorff-Heidepriem, "Progress in microstructured optical fibers," *Annu. Rev. Mater. Res.* **36**(1), 467–495 (2006).
23. S. H. Wemple, "Material dispersion in optical fibers," *Appl. Opt.* **18**(1), 31–35 (1979).
24. F. X. Gan, "Optical-Properties of Fluoride Glasses - a Review," *J. Non-Cryst. Solids* **184**, 9–20 (1995).
25. D. E. Zelmon, S. S. Bayya, J. S. Sanghera, and I. D. Aggarwal, "Dispersion of barium gallogermanate glass," *Appl. Opt.* **41**(7), 1366–1367 (2002).
26. T. Hasegawa, T. Nagashima, and N. Sugimoto, "Determination of nonlinear coefficient and group-velocity-dispersion of bismuth-based high nonlinear optical fiber by four-wave-mixing," *Opt. Commun.* **281**(4), 782–787 (2008).
27. G. Ghosh, "Sellmeier Coefficients and Chromatic Dispersions for Some Tellurite Glasses," *J. Am. Ceram. Soc.* **78**(10), 2828–2830 (1995).
28. T. Mito, S. Fujino, H. Takebe, K. Morinaga, S. Todoroki, and S. Sakaguchi, "Refractive index and material dispersions of multi-component oxide glasses," *J. Non-Cryst. Solids* **210**(2-3), 155–162 (1997).
29. W. S. Rodney, I. H. Malitson, and T. A. King, "Refractive index of Arsenic Trisulfide," *J. Opt. Soc. Am.* **48**(9), 633–636 (1958).
30. A. Mori, K. Kobayashi, M. Yamada, T. Kanamori, K. Oikawa, Y. Nishida, and Y. Ohishi, "Low noise broadband tellurite-based Er³⁺-doped fibre amplifiers," *Electron. Lett.* **34**(9), 887–888 (1998).
31. N. Sugimoto, T. Nagashima, T. Hasegawa, S. Ohara, K. Taira, and K. Kikuchi, "Bismuth-based optical fiber with nonlinear coefficient of 1360 W⁻¹km⁻¹," *Optical Fiber Communications Conference (OFC) 2004*, PDP26.
32. R. Mossadegh, J. S. Sanghera, D. Schaafsma, B. J. Cole, V. Q. Nguyen, P. E. Miklos, and I. D. Aggarwal, "Fabrication of single-mode chalcogenide optical fiber," *J. Lightwave Technol.* **16**(2), 214–217 (1998).
33. J. Ballato, T. Hawkins, P. Foy, R. Stolen, B. Kokuoz, M. Ellison, C. McMillen, J. Reppert, A. M. Rao, M. Daw, S. R. Sharma, R. Shori, O. Stafsudd, R. R. Rice, and D. R. Powers, "Silicon optical fiber," *Opt. Express* **16**(23), 18675–18683 (2008).
34. N. Healy, J. R. Sparks, M. N. Petrovich, P. J. A. Sazio, J. V. Badding, and A. C. Peacock, "Large mode area silicon microstructured fiber with robust dual mode guidance," *Opt. Express* **17**(20), 18076–18082 (2009).
35. A. S. Markus, G. Nicolai, W. Lothar, and R. Philip St, "Optical Properties of Chalcogenide-Filled Silica-Air PCF," in *Advances in Optical Materials*, OSA Technical Digest (CD) (Optical Society of America, 2009), AThD3.
36. M. A. Schmidt, N. Granzow, N. Da, M. Peng, L. Wondraczek, and P. S. J. Russell, "All-solid bandgap guiding in tellurite-filled silica photonic crystal fibers," *Opt. Lett.* **34**(13), 1946–1948 (2009).
37. X. Feng, F. Poletti, A. Camerlingo, F. Parmigiani, P. Horak, P. Petropoulos, W. H. Loh, and D. J. Richardson, "Dispersion-shifted all-solid high index-contrast microstructured optical fiber for nonlinear applications at 1.55 microm," *Opt. Express* **17**(22), 20249–20255 (2009).
38. X. Feng, T. M. Monro, P. Petropoulos, V. Finazzi, and D. Hewak, "Solid microstructured optical fiber," *Opt. Express* **11**(18), 2225–2230 (2003).
39. A. Camerlingo, X. Feng, F. Poletti, G. M. Ponzio, F. Parmigiani, P. Horak, M. N. Petrovich, P. Petropoulos, W. H. Loh, and D. J. Richardson, "Near-zero dispersion, highly nonlinear lead-silicate W-type fiber for applications at 1.55 microm," *Opt. Express* **18**(15), 15747–15756 (2010).
40. A. Camerlingo, F. Parmigiani, X. Feng, F. Poletti, P. Horak, W. H. Loh, D. J. Richardson, and P. Petropoulos, "Wavelength Conversion in a Short Length of a Solid Lead-Silicate Fiber," *IEEE Photon. Technol. Lett.* **22**(9), 628–630 (2010).
41. A. Camerlingo, F. Parmigiani, X. Feng, F. Poletti, P. Horak, W. Loh, D. Richardson, and P. Petropoulos, "Multichannel Wavelength Conversion of 40Gbit/s Non-Return-to-Zero DPSK Signals in a Lead Silicate Fibre," *IEEE Photon. Technol. Lett.* **22**(15), 1153–1155 (2010).
42. K. Kikuchi, K. Taira, and N. Sugimoto, "Highly nonlinear bismuth oxide-based glass fibres for all-optical signal processing," *Electron. Lett.* **38**(4), 166–167 (2002).
43. J. Y. Y. Leong, P. Petropoulos, J. H. V. Price, H. Ebendorff-Heidepriem, S. Asimakis, R. C. Moore, K. E. Frampton, V. Finazzi, X. Feng, T. M. Monro, and D. J. Richardson, "High-nonlinearity dispersion-shifted lead-silicate holey fibers for efficient 1 μm pumped supercontinuum generation," *J. Lightwave Technol.* **24**(1), 183–190 (2006).
44. D. Gloge, "Dispersion in weakly guiding fibers," *Appl. Opt.* **10**(11), 2442–2445 (1971).
45. D. Gloge, "Weakly guiding fibers," *Appl. Opt.* **10**(10), 2252–2258 (1971).

1. Introduction

The accurate control of the group velocity dispersion (GVD) profile of an optical fiber is paramount to the efficient exploitation of most fiber-based nonlinear optical effects. For example, a tailored dispersion profile is essential for the phase matching of parametric processes [1] or the control of soliton dynamics such as Raman soliton self frequency shifting [2], dispersive wave generation and trapping [3] or soliton spectral tunneling [4]; a zero dispersion wavelength (ZDW) close to the pump wavelength is also one of the prerequisites for efficient and broadband supercontinuum generation [5], where a good control of the fiber's GVD is also crucial to enhance the energy transfer to either shorter or longer wavelengths [6,7].

Major effort has therefore been devoted over the past several decades to develop technologies allowing fine control of the overall dispersion of optical fibers by modifying the waveguide dispersion (D_w) to counterbalance the intrinsic material dispersion of the optical glass (D_m). Historically, the first dispersion controlled fibers, including dispersion shifted, flattened and compensating fibers, were developed in the context of optical telecommunications to mitigate the adverse temporal pulse spreading induced by GVD in the newly discovered ultra low-loss third telecommunication window. The preform fabrication process, typically based on modified chemical vapor deposition (MCVD), allowed the creation of often complex refractive index profiles from a ultra-high purity silica glass host to create an optical waveguide with a controlled amount of waveguide dispersion. This technology was later on extended to the realization of smaller core fibers with flattened dispersion at telecoms wavelengths for nonlinear applications [8]. This well refined fabrication technology produces fiber preforms with a remarkably precise and reproducible radially symmetric refractive index profile, while the all-solid nature of these fibers ensures that such a profile is preserved from preform to fiber with an excellent stability of all structural dimensions along the fiber length. As a result, these fibers typically present well controllable and reproducible dispersion profiles, which also tend to have good stability along the longitudinal direction. The downside of this approach is that the maximum difference between core (n_{co}) and cladding (n_{cl}) refractive indices achievable through doping is typically low ($\Delta n_{max} = n_{co} - n_{cl} \sim 0.05$), which ultimately limits the amount of waveguide dispersion that can be introduced and prevents the overall dispersion of these fibers being radically different from the dispersion of the core glass. The maximum nonlinearity of these fibers is also quite small, typically limited to $\sim 30 \text{ W}^{-1}\text{km}^{-1}$.

A second, more recent method to achieve waveguidance and at the same time a broader range of dispersion profiles, requires the incorporation of longitudinal air holes in the cross section of single-glass fibers, known as holey fibers (HFs) or photonic crystal fibers (PCFs) [9]. The much higher refractive index contrast between glass and air, ranging from the ~ 0.45 of silica structures to more than 2 for glasses made of heavier constituent atoms, and the vast freedom in the choice of shape, size and topology of the holes, results in much higher values of fiber nonlinearity together with an unprecedented level of control of the dispersive properties. HFs with a ZDW down to the visible region of the spectrum [10], two or even three ZDWs at tailored spectral positions [4,11], or a flat dispersion region extending over a bandwidth of several hundred nanometers have all been reported [12–15]. However, producing holey structures with the required structural precision in both transverse and longitudinal directions to reliably and reproducibly achieve a desired dispersion profile has proven much more difficult than for all-solid, low index contrast fibers. Temperature gradients within the fiber furnace, coupled with different surface tensions and gas pressures experienced by holes with dissimilar size, typically tend to create unpredictable structural distortions when drawing a preform down to the size of a cane or a fiber. Such distortions are difficult to control or pre-compensate, and as a result it is extremely challenging to obtain an accurate and reproducible dispersion profile in a highly nonlinear HF [16].

In this work we propose and demonstrate a third alternative method to obtain dispersion controlled fibers with a high value of effective nonlinearity, where two or three high refractive

index glasses with large index contrast (Δn ranging from 0.05 to more than 2) are combined in an all-solid, circularly symmetric geometry. Such fibers provide at the same time an excellent fabrication reproducibility and stability, and a highly tailorable dispersion control, thus combining the best qualities of low contrast, all-solid conventional fibers with those of high contrast HFs. Furthermore, through simultaneous use of high Δn and small core sizes, they can typically achieve extremely high values of nonlinearity, as required for nonlinear applications, where simpler pumps at lower peak powers or shorter fiber lengths less prone to longitudinal fluctuations of diameter and hence dispersion can be used.

Here we present general design rules and a simple algorithm to design high index contrast, step-index fibers (SIFs) with an arbitrary value of dispersion (D) and dispersion slope (DS) at a selected wavelength within the transparency window of the core glass. We study the singlemode operation regime of these fibers and propose the introduction of a second outer cladding to strip off the few high order modes present at shorter wavelengths and thus obtain an effectively singlemode operation. We then apply the proposed rules to the design of dispersion flattened fibers (zero D and DS at a given wavelength) and of fibers for supercontinuum generation. Finally, in order to prove the potential of such a novel fiber design concept, we discuss the design and fabrication of a recently reported highly nonlinear dispersion flattened fiber.

The paper is organized as follows: Section 2 reviews the waveguide and total dispersion properties of high index SIFs; Section 3 proposes an optimization algorithm to design a SIF made from an arbitrary glass and exhibiting desired values of D and DS at a given wavelength. Section 4 and 5 discuss issues related to the choice of the glasses and present an example of a fabricated highly nonlinear, single mode, dispersion flattened fiber based on the proposed design approach. Section 6 presents a few further examples of dispersion controlled fibers obtained with the previous algorithm, while Section 7 summarizes the work.

2. Dispersion of circularly symmetric, high index contrast SIFs

To understand the proposed fiber design approach, it is instructive to study the waveguide dispersion of a simple step-index fiber when the contrast between core and cladding refractive indices is large. For all fibers in this work we assume a circular radial symmetry, which is useful since it allows the use of semi-analytical calculation methods to simplify the numerical analysis, but not essential. Using an extrusion-based fabrication approach for example, fibers without circular symmetry could be obtained, which may represent a future extension of the method presented here [17].

For large refractive index differences, the weakly guiding approximation commonly used for the description of mode propagation in conventional optical fibers cannot be applied. The exact solution of Maxwell's equation for the hybrid fundamental HE_{11} leads to the following, well known, characteristic equation [18]:

$$\left[\frac{J_1'(U)}{UJ_1(U)} + \frac{K_1'(W)}{WK_1(W)} \right] \left[\frac{J_1'(U)}{UJ_1(U)} + \left(\frac{n_{cl}}{n_{co}} \right)^2 \frac{K_1'(W)}{WK_1(W)} \right] = \left(\frac{n_{eff}}{n_{co}} \right)^2 \left(\frac{1}{W^2} + \frac{1}{U^2} \right) \quad (1)$$

where n_{eff} is the effective index, J_1 , K_1 , J_1' and K_1' are the 1st order Bessel functions of the first and second kind and their derivatives, respectively, and U and W are the transverse wave numbers, related to the wavelength (λ), fiber diameter (d) and effective index by $U = \pi d / \lambda \sqrt{n_{co}^2 - n_{eff}^2}$, $W = \pi d / \lambda \sqrt{n_{eff}^2 - n_{cl}^2}$. Solving Eq. (1) for a given SIF at different wavelengths (i.e. for given values of $n_{co}(\lambda)$, $n_{cl}(\lambda)$, and d) returns the wavelength dependence of its effective index, $n_{eff}(\lambda)$. If the material dispersion of the constituent glasses is included when solving Eq. (1), numerical differentiation of n_{eff} gives the total dispersion of the fiber:

$$D(\lambda) = -\frac{\lambda}{c} \frac{d^2 n_{eff}(\lambda)}{d\lambda^2}. \quad (2)$$

Alternatively, if the material dispersion is at first neglected and the characteristic Eq. (1) is solved with $n_{co}(\lambda) = n_{co}(\lambda_t)$ and $n_{cl}(\lambda) = n_{cl}(\lambda_t)$ for a given λ_t , Eq. (2) will yield the *waveguide* dispersion of the fiber $D_w(\lambda)$. The total dispersion can then be approximately calculated from

$$D(\lambda) \approx D_w(\lambda) + D_m(\lambda), \quad (3)$$

where for fibers with high modal confinement in the core the material dispersion contribution $D_m(\lambda)$ can be well approximated by the material dispersion of the core glass. This second approximate method has the advantage of clearly separating the *waveguide* contribution from the *material* contribution to the overall dispersion, which is useful in the fiber design stage, as will be shown below. The approximations introduced by neglecting (i) the wavelength dependence of the index contrast and (ii) the material dispersion of the cladding glass, typically result in only small percentage errors in the overall calculated dispersion, which can be either tolerated or corrected through an additional design iteration (see Section 3).

As an illustrative example, Eq. (1) is solved with this second method for a range of SIFs to show the dependence of $n_{eff}(\lambda)$, $D_w(\lambda)$ and $D(\lambda)$ on the structural parameters d and Δn . The left column in Fig. 1 shows the effect of a diameter change for a fixed Δn , while the right column shows the effect of changing Δn when d is fixed. Note that although for these calculations we have assumed specific structural values, approximately corresponding to those of the fabricated dispersion flattened fiber discussed in Section 5 ($n_{co} = 1.80$, $n_{cl} = 1.52$ and $d = 1.7 \mu\text{m}$), the general conclusions drawn from Fig. 1 are valid for any other set of parameters.

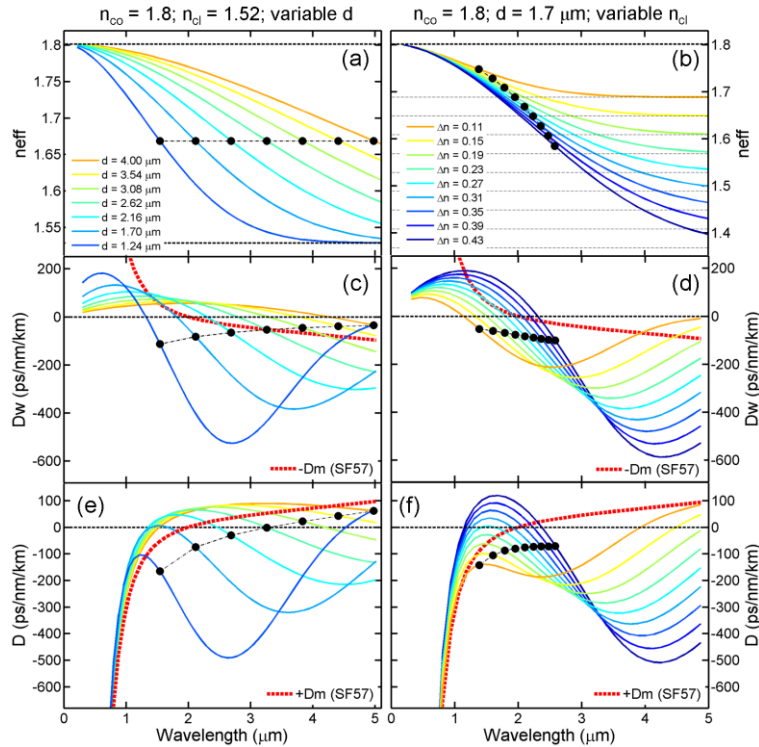


Fig. 1. Wavelength dependence of effective index (n_{eff}), waveguide dispersion (D_w) and total dispersion (D) for step index fibers with an SF57 glass in the core and: variable core diameter d with $\Delta n = 0.28$ (left column) and variable Δn with $d = 1.7 \mu\text{m}$ (right column).

Figures 1(a) and 1(b) show that, as is well known, n_{eff} tends to n_{co} for vanishingly small wavelengths ($\lambda \ll d$), and to n_{cl} for $\lambda \gg d$. As a result, the waveguide dispersion contribution is negligible in both the short and long wavelength limit, Figs. 1(c) and 1(d). For any practical optical wavelength in between, D_w assumes an approximately sinusoidal wavelength

dependence, going from a positive (anomalous) contribution at shorter wavelengths to a negative (normal) contribution at longer wavelengths. The key point to observe here is that the waveguide dispersion *slope* (DS_w) is to good approximation only influenced by changes in diameter (where smaller diameters generate larger slopes, as is seen in Fig. 1(c)), while a change in index contrast shifts the D_w curves with respect to wavelength (larger Δn shifts the curves towards longer wavelengths) and compresses/expands them vertically, but leaves their slope nearly unchanged, Fig. 1(d). A similar behavior has been previously observed in HFs, where changing the hole-to-hole spacing is equivalent to scaling d for SIFs, while modifying the air filling fraction acts like a change in Δn [19].

To appreciate the effects that a change in d or Δn will have on the *total* dispersion, it is instructive to overimpose the *material* dispersion curve, taken with a negative sign ($-D_m$), to the D_w curves previously calculated. In the example in Figs. 1(c) and 1(d), the material dispersion of the core glass (SF57, a commercially available lead silicate, $n = 1.80$ at $1.55 \mu m$ [20]) is shown as a dashed red line. Obviously, the points where D_w and $-D_m$ intersect correspond to ZDWs in the total profile; at those wavelengths where $D_w > -D_m$ the total dispersion is anomalous, while elsewhere it is normal, as shown in Figs. 1(e) and 1(f). From the previous empirical observations on the dependence of D_w and DS_w on the structural parameters of a SIF it is now straightforward to derive a simple recipe to design fibers with a desired value of waveguide dispersion *and* waveguide dispersion slope at a given wavelength: first (i) for a given core glass and an arbitrary initial choice of cladding refractive index the fiber diameter is tuned to generate the desired total dispersion slope; then (ii) Δn is adjusted to match the required absolute dispersion, with little influence on the slope determined in (i).

The number of modes guided in these fibers also deserves some attention, since singlemode guidance is highly preferable or even mandatory for many applications. The black circular markers in Fig. 1 show the numerically calculated cut-off wavelength λ_{co} of each fiber design, indicating that at wavelengths shorter than the marker the fibers do support multiple modes. Figures 1(a) and 1(b) show that the single mode condition approximately occurs for $n_{eff} \sim (n_{co} + n_{cl})/2$. Most importantly though, Figs. 1(c) and 1(d) show that fibers are always multimoded when their waveguide dispersion contribution is anomalous, which we verified numerically also for a broad range of other SIF designs. This means that whenever a SIF presents a ZDW at wavelengths shorter than the zero *material* dispersion wavelength (ZMDW), which is only possible through some anomalous waveguide dispersion contribution, the fiber will certainly be multimoded at that wavelength, Figs. 1(e) and 1(f). Therefore, simple SIFs with low absolute value of dispersion at wavelengths shorter than the ZMDW cannot be strictly single moded, which may prevent their use in applications such as all optical signal processing of telecoms data or supercontinuum-generation. As we will show in more detail through the example of a fabricated fiber in Section 5, a simple and effective way to restore effectively single mode guidance without perturbing the dispersive properties of a SIF is to introduce a second outer cladding with a refractive index n_{ocl} between n_{co} and n_{cl} , thereby generating a W-shaped refractive index profile. Since high order modes (HOMs) have a larger fraction of the electromagnetic field in the cladding as compared to the fundamental mode (FM) [18], see also Fig. 6(a), by carefully optimizing n_{ocl} and the diameter of the outer cladding region d_{ocl} , a high leakage loss can be introduced for all HOMs, while leaving the loss and dispersive properties of the FM almost unperturbed.

It is finally worth stressing that, as already observed by Ferrando et al. [19], the dimensionless nature of the effective index implies that its dependence on the structural parameters can only occur through dimensionless ratios, i.e. $n_{eff} = n_{eff}(d/\lambda, n_{co}, n_{cl})$. Therefore for any real scaling factor $M \neq 0$ we can obtain a *scaling rule* for the waveguide dispersion:

$$D_w(M \cdot d, \lambda, n_{co}, n_{cl}) = \frac{1}{M} D_w(d, \lambda / M, n_{co}, n_{cl}). \quad (4)$$

As a result, once a waveguide dispersion curve is known for a specific combination of d , n_{co} and n_{cl} , it is possible to obtain D_w for any other particular fiber diameter of interest by appropriately stretching the curve, without the need to recalculate Eq. (1). Note also that the

1/M scaling factor implies that smaller cores generate higher absolute values of waveguide dispersion (shifted to shorter wavelengths), as shown in Fig. 1(c).

3. Automatic dispersion optimization routine

In the previous section we have indicated simple empirical rules to design a step-index fiber with a desired dispersion at a particular wavelength. Here we present a numerical routine that based on these rules automatically determines the optimum structure without any need for cumbersome manual intervention. The algorithm is formed by two nested optimization loops, each of which finds the optimum value of one variable to minimize a smooth error function. For this task, any simple numerical optimization routine, e.g. based on gradient descent, Newton's method, Nelder-Mead downhill simplex method [21], or even evolutionary techniques [15] can be employed. The algorithm is the following:

1. Choose the wavelength of operation λ_t and a high refractive index glass to be used in the core. This will determine a value of core index $n_{co}(\lambda_t)$ which will not change throughout the procedure, making each SIF design dependent only on diameter and index difference, $\{d, \Delta n(\lambda_t)\}$. For simplicity of notation, in the following steps the explicit wavelength dependence of all variables will be dropped and all calculated values will be implicitly referred to the target wavelength λ_t .
2. Select a target value of dispersion D_t and dispersion slope DS_t at λ_t , from which the target *waveguide* dispersion $D_{wt} = D_t - D_m$ and *waveguide* dispersion slope $DS_{wt} = DS_t - DS_m$ can be obtained. Choose a desired accuracy on the values of dispersion (ϵ_D) and dispersion slope (ϵ_{DS}).
3. Choose initial guess values of fiber diameter and index difference $\{d^{(0)}, \Delta n^{(0)}\}$, which will also obviously determine $n_{cl}^{(0)} = n_{co}^{(0)} - \Delta n^{(0)}$. Here the superscript numbers indicate the progressive step in the algorithm. Note that this initial choice will have an influence on the number of steps required by the algorithm to converge, but will not generally prevent its convergence (see the example in Fig. 2). Calculate the waveguide dispersion curve of this initial fiber through Eq. (1) and evaluate $D_w^{(0)}$ and $DS_w^{(0)}$ at λ_t . Note that although these quantities need to be evaluated at one wavelength, in order to be able to apply the scaling rule in the next step, calculation of D_w over a broad enough wavelength range around λ_t is required.
4. Through a numerical optimization routine and using the scaling rule in Eq. (4), modify d until a new value of diameter $d^{(1)}$ is found such that $DS_{err}^{(1)} = |DS_w^{(1)} - DS_{wt}| < \epsilon_{DS}$. The structure $\{d^{(1)}, \Delta n^{(0)}\}$ will have a dispersion slope at λ_t well matched to the target one, but some residual error in the absolute value of waveguide dispersion, $D_{err}^{(1)} = |D_{wt} - D_w^{(1)}|$.
5. Modify the index difference to $\Delta n^{(1)}$, recalculate the waveguide dispersion through Eq. (1) with $\{d^{(1)}, \Delta n^{(1)}\}$ and repeat step 4 to obtain a new optimum diameter $d^{(2)}$ such that, again, $DS_{err}^{(2)} = |DS_w^{(2)} - DS_{wt}| < \epsilon_{DS}$. Estimate $D_{err}^{(2)} = |D_{wt} - D_w^{(2)}|$, for $\{d^{(2)}, \Delta n^{(1)}\}$.
6. Through a numerical optimization routine applied to step 5, modify Δn until, after n steps, the desired combination of diameter and index contrast $\{d^{(n+1)}, \Delta n^{(n)}\}$ is found such that, at the same time, $D_{err}^{(n+1)} < \epsilon_D$ and $DS_{err}^{(n+1)} < \epsilon_{DS}$.

Figure 2 shows two examples of dispersion optimization using this algorithm, where the optimization loops have been implemented using the simplex method. In both examples the core glass is SF57 and the targets are $D_t = 0$ ps/nm/km and $DS_t = 0$ ps/nm²/km at $\lambda_t = 1.55$ μ m. ϵ_D and ϵ_{DS} are set to 0.01 ps/nm/km and 10^{-6} ps/nm²/km, respectively. Two rather different initial guesses for $\{d^{(0)}, \Delta n^{(0)}\}$ have been chosen to demonstrate the convergence of the algorithm and the independence of the results from the initial guess: $\{4$ μ m, 0.25 $\}$ is shown in Fig. 2(a) while $\{1.3$ μ m, 0.4 $\}$ is used in Fig. 2(b). The waveguide dispersion of these starting

fibers is shown by the pink dash-dot line. As can be seen, both optimizations converge towards the same optimum result, $d = 1.78 \mu\text{m}$, $\Delta n = 0.26$ (black curves). Less than 20 total optimization steps and a computation time of less than a minute on a standard PC are required.

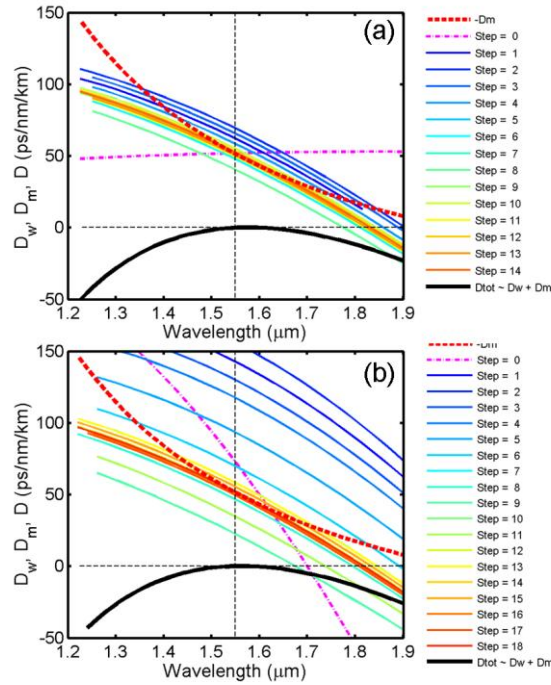


Fig. 2. Optimization steps in the automatic design of a dispersion flattened SIF. The material dispersion ($-D_m$) of the SF57 core is shown by the red dashed line. Optimization targets are $D_t = 0 \text{ ps/nm/km}$ and $DS_t = 0 \text{ ps/nm}^2/\text{km}$ at $\lambda_c = 1.55 \mu\text{m}$. Initial $\{d^{(0)}, \Delta n^{(0)}\}$ conditions are: (a) $\{4 \mu\text{m}, 0.25\}$; (b) $\{1.3 \mu\text{m}, 0.4\}$. Both optimizations reach the same optimum fiber with $d = 1.78 \mu\text{m}$ and $\Delta n = 0.26$, and the optimum total dispersion is shown by the black line.

The procedure presented above relies on two main assumptions: (i) calculating the dispersion as a sum of material and waveguide dispersion as in Eq. (3) does not introduce significant errors and (ii) the waveguide dispersion of the cladding can be neglected. In order to check the validity of these assumptions, we use the optimum fiber from the previous example. Figure 3 shows its dispersion curves, calculated with either the approximate method of Eq. (3) (red curve) or with the more accurate direct inclusion of the material dispersion into Eq. (1) (cyan curve). As can be seen, the flatness at the target wavelength is maintained and the two curves are very similar, apart from a small vertical displacement. For the more rigorous calculation, the desired target value of $D_t = 0 \text{ ps/nm/km}$ could be restored, for example, by reducing the core diameter by just $\sim 1\%$. The blue curve, finally, shows the effect of considering the wavelength dependence of a real cladding. Here we have chosen another lead silicate glass, LLF1 [20], which has a refractive index difference with the core glass (SF57) of $\Delta n = 0.273$ at $1.55 \mu\text{m}$, not too distant from the theoretical design requirement of $\Delta n = 0.255$. By slightly reducing the core diameter to $1.68 \mu\text{m}$ in order to compensate for the higher Δn , a curve close to the design target (but with a small, nonzero dispersion slope at $1.55 \mu\text{m}$) is once again achieved, demonstrating that (i) the approximations introduced are sensible, (ii) the design procedure discussed in the previous section provides an excellent first approximate solution for the design of a real fiber and (iii) a final simulation including the material dispersion of all glasses is probably needed in the end to fine tune the target dimensions.

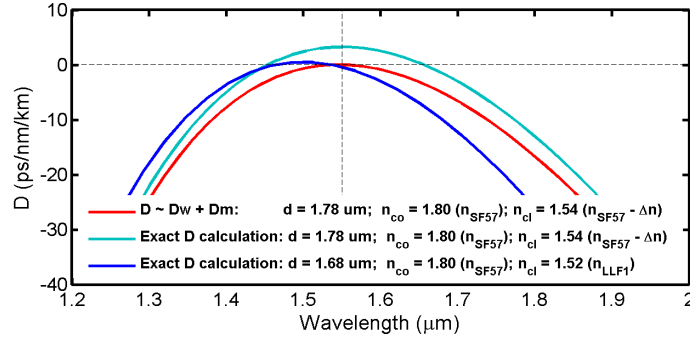


Fig. 3. Calculated dispersion of the optimum fiber in Fig. 2, obtained by: approximate method of Eq. (3) (red); direct inclusion of the core material dispersion in Eq. (1) with a constant Δn (cyan); direct inclusion of the material dispersion of two real glasses as a core (SF57) and cladding (LLF1) media (blue).

4. Choice of core and cladding glasses

Having presented and validated a fiber design process to tailor the dispersive properties of all solid SIFs with high index contrast, in this section we add a few comments on the choice of suitable glasses and on possible fabrication approaches to realize such structures. A detailed discussion of the main optical, thermal and mechanical properties of the glasses commonly used in the fabrication of highly nonlinear fibers is outside the scope of this work. And for this the reader is referred to the works in refs [7,22] and in references therein.

For high contrast SIFs operating at wavelengths close to or shorter than the first high order mode cut-off wavelength (circular markers in Fig. 1) the fraction of power guided in the core is typically larger than 85-90% [18]. Therefore, the most critical choice in the entire fiber design procedure regards the glass to be employed in the core. Not only will this glass have a direct influence on the transparency range, nonlinearity and ultimate loss of the dispersion controlled fibers, but through its material dispersion it will also indirectly determine the number of guided modes (and thus whether or not a second outer cladding is required), and the bandwidth of the dispersion controlled region.

The material dispersion of any transparent solid is directly related through the Kramers-Kronig equations to the position and strength of its electronic absorptions in the UV/visible and its vibrational absorptions in the mid-IR. A simplified two-pole Sellmeier equation can be used to derive the material dispersion at wavelengths shorter than the phonon resonances [23]:

$$n^2(\omega) - 1 = E_d E_o / (E_o^2 - \hbar^2 \omega^2) - E_l^2 / \hbar^2 \omega^2 \quad (5)$$

where ω is the optical frequency. The first term on the right hand side represents the contribution from electronic absorptions (with E_o denoting a mean electronic energy gap and E_d the corresponding oscillator strength, both in eV), while the second term comes from the lattice vibrations (with E_l being a measure of the lattice oscillator strength). The position of the ZMDW λ_0 , whose offset with respect to the operational wavelength has a paramount influence on the final properties of these dispersion controlled fibers, as we shall see, typically lies somewhere in the middle of the spectral transparency range (see Fig. 4) and can then be estimated from [23]:

$$\lambda_0(\mu m) = 1.63(E_d / E_o^3 E_l^2)^{1/4}. \quad (6)$$

The inverse dependence of λ_0 on E_o indicates a rapid increase of the ZMDW in materials with a lower average electronic energy gap. Table 1 shows typical values of ZMDW for various families of glasses, where λ_{elec} and λ_{phon} are the wavelengths of the main electronic and vibrational absorption peaks, respectively.

Table 1. ZMDW of various families of optical glasses

	Glass	λ_{elect} (μm)	ZMDW λ_0 (μm)	λ_{phon} (μm)
Low refractive index ($n < 1.7$)	Silica	< 0.2	1.27	< 5
	Fluorides	< 0.2	1.5 – 1.7	5 – 10
	Heavy metal oxides, silicate based	0.3 – 0.4	~ 2	< 5
High refractive index ($n > 1.7$)	Heavy metal oxides non-silicate based: e.g., tellurite, germanate, gallate	0.3 – 0.7	2 – 3	5 – 10
	Chalcogenides	0.6 – 0.9	5 – 7	> 10

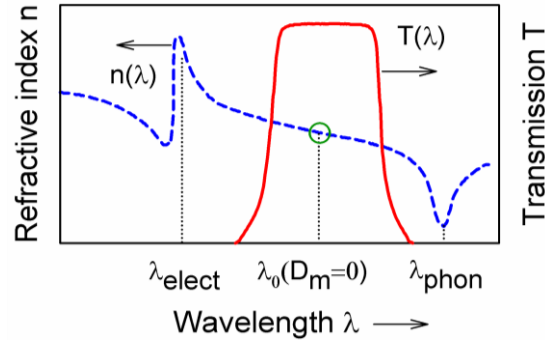


Fig. 4. Typical dispersion and transmission curves of a glass

Despite these large differences in ZMDW, however, the vast majority of optical glasses amenable to fiber fabrication share a qualitatively similar material dispersion wavelength dependence, which is well exemplified by the D_m curve of SF57 shown in Fig. 1(e) and shown for several other glasses in Fig. 5. As can be seen, the ZMDW typically separates two qualitatively different regions: at wavelengths much shorter than the ZMDW, $D_m(\lambda)$ is very steep and normal, while at wavelengths longer than the ZMDW, $D_m(\lambda)$ is anomalous with a much shallower and in most cases close to linear wavelength dependence.

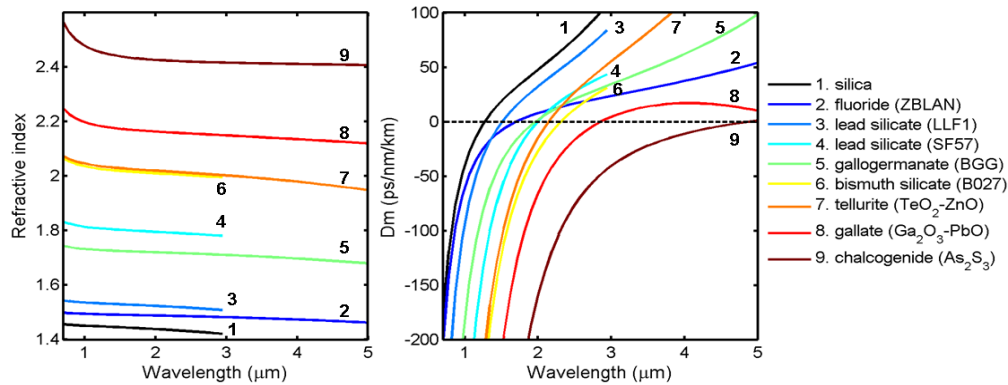


Fig. 5. Refractive index (left) and material dispersion (right) of some common optical glasses: 1. silica [1]; 2. ZBLAN [24]; 3. and 4. Schott lead silicates [20]; 5. barium gallogermanate [25]; 6. bismuth silicate [26]; 7. zinc tellurite [27]; 8. lead gallate [28]; arsenic trisulfide [29].

Generally, from Fig. 5 it is evident that in order to have some sort of dispersion control at wavelengths *much shorter* than the ZMDW, large values of anomalous dispersion are required. From the behavior highlighted in Fig. 1(c) this can only be obtained with small enough fiber diameters. Small core diameters however also shift the D_w curves to short

wavelengths, see the scaling rule in Eq. (4), and this must be compensated by using larger values of Δn , see Fig. 1(d). In contrast, at wavelengths *close* to or *longer* than the ZMDW, larger core diameters and hence smaller Δn are sufficient to achieve a waveguide dispersion contribution similar in magnitude and opposite in sign to the material one. Therefore, based on the choice of core glass and on where its ZMDW is positioned with respect to the intended operational range of the fiber, significantly different values of d and Δn can be expected, which ultimately also influence the most suitable fabrication approach to be adopted.

Dispersion controlled fibers operating at wavelengths larger than the ZMDW and requiring smaller index contrasts (e.g. $\Delta n \sim 0.05$ -0.2) are most likely to be based on glasses of the same family, with tailored compositional variations. For example, SIFs with core and cladding made of tellurite [30], bismuth [31] or chalcogenide [32] based glasses of slightly different compositions have been already demonstrated, although in all these cases no attempt was ever made to control the overall fiber dispersion, as we suggest in this work.

If dispersion control is required at wavelengths much shorter than the ZMDW, on the other hand, the larger Δn required may or may not be achievable through glasses of the same family. The fabricated lead silicate fiber presented in the next section is an example of a high Δn fiber ($\Delta n = 0.27$) achieved with glasses of the same family, while several reported examples of fibers with a silica clad and a semiconductor core (either amorphous, crystalline or polycrystalline) clearly demonstrate that widely different optical materials with a high Δn can coexist in the same fiber [33–35].

In case a third glass is required in the outer cladding to enforce singlemode operation, a much greater freedom exists in the choice of its properties. In this case, thermo-mechanical compatibility with the other two glasses should be the main factor determining the glass choice, and the outer diameter d_{ocl} can be used as an additional free parameter to tailor the differential mode loss (see Section 5).

Different fabrication methods have been reported so far to realize high index contrast step-index fibers, for example the double crucible technique [32], the Taylor wire method [33], the high pressure chemical vapor deposition technique [34], the pumping of molten glasses inside silica templates [35,36] or the extrusion, drilling and stacking technique [16]. The most suitable method will in general depend on the particular combination of glasses involved and whether or not a second cladding is required. In any case, in order to fabricate robust fibers, particular attention has to be devoted to the thermal, chemical and mechanical compatibility of all the glasses involved, a discussion of which is beyond the scope of this paper.

5. Fabricated dispersion flattened fiber with a W-type refractive index profile

In the past few years we have developed and perfected a fabrication technique for soft glass fibers based on extrusion and stacking, which has been successfully applied to the fabrication of all-solid fibers made of two different glasses [37,38]. Using the same approach, we have also recently fabricated a W-index profiled dispersion flattened fiber for all-optical processing of telecoms data, following the design prescriptions of this work. A detailed discussion of its fabrication and characterization has already been presented [39]. Here we will expand on its design concept, showing how it straightforwardly follows from the design rules previously discussed, summarize its main properties and present an improved design.

The target in this work was a highly nonlinear, singlemode and dispersion flattened fiber (DS ~ 0 ps/nm²/km) with an absolute value of dispersion below 5 ps/nm/km for all-optical wavelength conversion and regeneration in the 1.55 μm wavelength region. The commercially available glass Schott SF57 was chosen as a core material due to its relatively high linear and nonlinear refractive indices and good thermal stability. As shown in Fig. 1, modeling indicated that the dispersion targets would be met by a fiber with approximately $d = 1.7 \mu\text{m}$ and $\Delta n = 0.27$. After a search for a compatible and commercially available glass presenting an index contrast close to this target, we decided to employ in the cladding another lead silicate, LLF1, providing $\Delta n = 0.273$ at 1.55 μm . Since SF57 has a ZMDW at around 2 μm , such a SIF would be multimoded at telecoms wavelengths (see Section 2). Therefore, we performed finite element method simulations of various W-type fibers to select a glass for the outer

cladding and optimize its diameter to generate a significantly high confinement loss for the LP_{11} mode (e.g. > 50 dB/m) without affecting the loss and dispersion of the LP_{01} mode. We observed that with a careful choice of the outer cladding diameter several glasses could be used for this task. For fabrication compatibility we finally opted for a third glass of the same lead silicate family, SF6 ($n = 1.76$ at $1.55 \mu\text{m}$). As shown in Fig. 6(b), the choice of a d_{ocl}/d ratio around 4.5 produces a differential mode loss of more than three orders of magnitude, sufficient to create effectively singlemode guidance without altering the dispersive properties of the fundamental mode of the inner step-index waveguide.

Using a room temperature drill, polish and stacking technique for the two inner cylindrical regions of the fiber, and extrusion for the outer cladding, we obtained a cane with the desired d_{ocl}/d ratio of 4.54. This ratio was exactly maintained when the cane was subsequently drawn down to fiber dimensions, and several bands with excellent longitudinal stability but slightly different outer diameters were obtained. The fiber shown in Fig. 6(c) has $d = 1.63 \mu\text{m}$ and $d_{\text{ocl}} = 7.4 \mu\text{m}$, which generate the flat and slightly normal dispersion profile shown in Fig. 6(d), measured with an interferometer using a supercontinuum source [39]. The effective area, nonlinear coefficient and propagation loss of the fiber were $1.9 \mu\text{m}^2$, $820 \text{ W}^{-1}\text{km}^{-1}$ and 2.1 dB/m , respectively. Note that this value of loss is close to the bulk loss of the core glass and is mostly due to a relatively high residual level of impurities in the commercial glass. Purer glasses are expected to exhibit 1-2 orders of magnitude lower losses, which would make these fibers even more appealing for nonlinear-based applications. Nonlinear absorption is negligible at telecoms wavelengths for lead silicate glasses. As expected, an effectively single mode behavior was observed even after transmission over just one meter of fiber [39]. Note that, as shown in Fig. 6(d), by using fiber with a marginally larger core (e.g. $+2\%$), slightly anomalous and flat dispersions is also achievable.

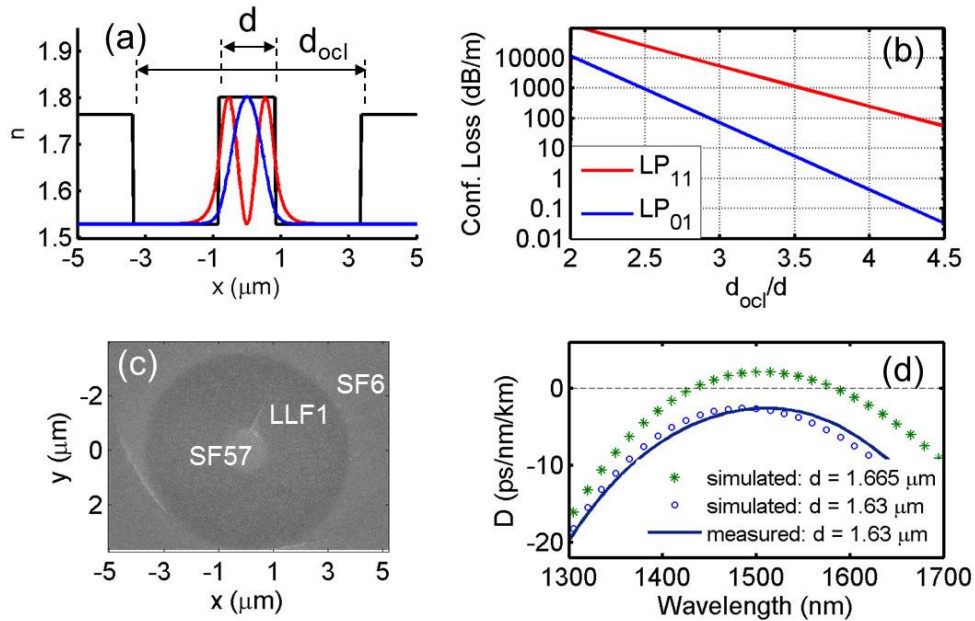


Fig. 6. (a) Refractive index and modal profiles of the fabricated dispersion flattened fiber. The core, cladding and outer cladding glasses are all Schott lead silicates (SF57, LLF1 and SF6, respectively). $d = 1.63 \mu\text{m}$; $d_{\text{ocl}} = 7.4 \mu\text{m}$; (b) calculated confinement loss of the two core guided modes as function of d_{ocl}/d ratio at $1.55 \mu\text{m}$; (c) SEM of the fabricated fiber; (d) simulated and measured group velocity dispersion.

As already shown by a number of experiments, this fiber has extremely promising properties for all-optical processing applications [40,41]; its simple fabrication process and

the accuracy achieved in the control of its structural and dispersive properties fully demonstrate the potential of the novel fiber concept proposed in this work.

Additional simulations indicate that by using glasses with even higher nonlinear refractive indices it should be possible to achieve a significant improvement in the total value of nonlinearity, while maintaining single modality and a similarly flat dispersion profile. For example, by using a bismuth oxide based glass ($n = 2.02$ at $1.55 \mu\text{m}$ [42]) surrounded by two concentric lead silicate claddings made of SF2 and SF57 ($n = 1.62$ and 1.80 , respectively [20]) with $d = 1.37 \mu\text{m}$ and $d_{\text{ocl}} = 4d$, a three times higher nonlinearity of $\gamma = 2600 \text{ W}^{-1}\text{km}^{-1}$ could be achieved in a singlemode, dispersion flattened fiber. Such a fiber would represent a remarkable improvement over the nonlinear and dispersive properties of state-of-the-art highly nonlinear Bismuth fibers ($\gamma \sim 1200 \text{ W}^{-1}\text{km}^{-1}$ and $D = -270 \text{ ps/nm/km}$) [26].

6. Further examples of dispersion tailored fiber designs

As already shown, the position and offset of the ZMDW of the core glass with respect to the operational wavelength have an influence on the overall *nonlinearity* of these dispersion controlled fibers. From the scaling rule in Eq. (4) one would expect it also to affect the *bandwidth* of the dispersion controlled region, with narrower bandwidths achievable at shorter wavelengths. To confirm this prediction, in Fig. 7 we present four different fiber designs obtained with the previously discussed algorithm. In this example the core glass is, once again, SF57. The dispersion targets were set as $D_t = 3 \text{ ps/nm/km}$ and $DS_t = 0 \text{ ps/nm}^2/\text{km}$ at $\lambda_t = 1.05, 1.55, 2$ and $2.5 \mu\text{m}$, respectively. The optimum values for d and Δn for all fibers are reported in the figure and confirm the expected trend of larger diameters and smaller index contrasts required as the wavelength of interest λ_t is increased. These simulations show the flexibility of the proposed method in tailoring the overall dispersion. They also illustrate how the spectral width of the flat dispersion region increases with λ_t , as a result of the fact that shorter wavelengths require higher values of D_w , hence a smaller d , resulting in a narrower spectral region of anomalous waveguide dispersion, see Eq. (4). At wavelengths close to or longer than the ZMDW it is possible to engineer D_w to match the absolute value and slope of D_m over very broad bandwidths, in some cases exceeding a full octave, allowing flat and ultrawide bandwidth dispersion designs. Demonstrations of this concept have already been provided, for example, by various silica HFs [12,14,15,19].

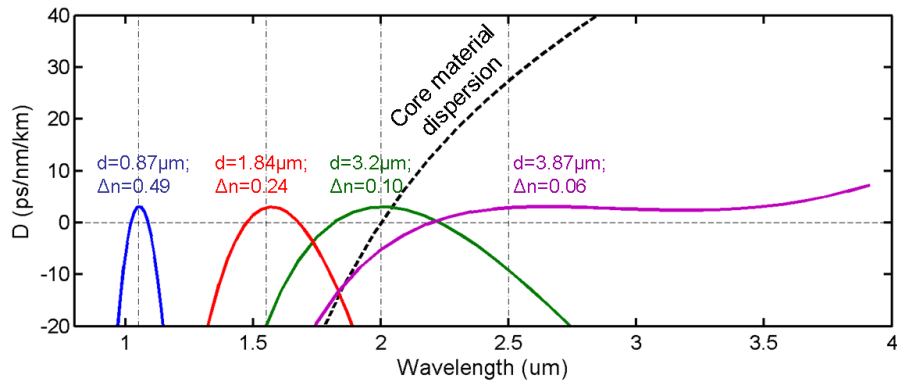


Fig. 7. Example of dispersion flattened designs ($DS_t = 0 \text{ ps/nm}^2/\text{km}$) at four different wavelengths: $1.05, 1.55, 2$ and $2.5 \mu\text{m}$. The core material is Schott SF57 and the optimum value of diameter and index contrast are indicated next to each curve.

It is worth stressing that due to the particular choice of core glass not all the 4 designs in this example are of practical significance. The fiber for $2.5 \mu\text{m}$ operation, for example, would have limited scope due to the poor mid IR transmission of silicate-based glasses. In this case, non-silicate glasses with longer phonon absorption edge should be used, as shown later on. Moreover, the dispersion flattened fiber at $\lambda_t = 1.05 \mu\text{m}$ would require a cladding with

$n_{cl} \sim 1.32$, typical of a liquid rather than a solid medium, suggesting that a SF57 micro-rod immersed in a liquid or, more practically, a liquid filled wagon wheel fiber [43], would produce the desired dispersion.

In Fig. 8 we provide two additional examples of dispersion controlled fiber designs obtained through the proposed method. Rather than dispersion flattened fibers, here we target fibers with dispersive profiles suitable for efficient and wide-bandwidth supercontinuum generation, where a ZDW must be positioned close to the pump wavelength and an anomalous dispersion region at longer wavelengths is beneficial to exploit soliton dynamics [5]. Figure 8(a) shows the calculated dispersion of a fiber for mid-IR supercontinuum generation from a 2 μm pump. The core material, a tellurite glass (TeO_2 based, $n = 1.994$ at 2 μm [27]), was chosen for its long infrared absorption edge; the target D_t was set to 0 ps/nm/km at $\lambda_t = 2$ μm , while $DS_t = 0.05$ ps/nm²/km was optimized to provide an octave spanning region of flat dispersion. The optimum fiber, with $|D| < 10$ ps/nm/km between 1.8 and 4.5 μm , has $d = 2.82$ μm and an index difference $\Delta n \sim 0.15$ at 2 μm , which seems achievable through moderate compositional modifications of the core glass [27].

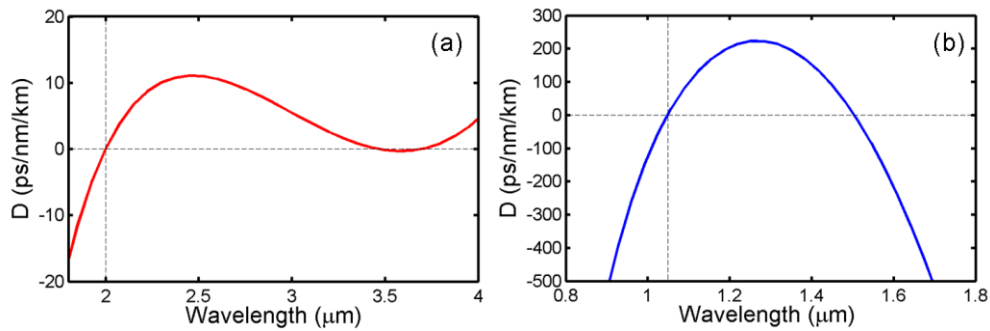


Fig. 8. Two examples of dispersion tailored fibers for supercontinuum generation. (a) tellurite fiber, $d = 2.82$ μm , $n_{co} = 1.994$, $n_{cl} = 1.840$ at $\lambda_t = 2$ μm . (b) silica fiber with a GLS core, $d = 0.68$ μm , $n_{co} = 2.395$, $n_{cl} = 1.450$ at $\lambda_t = 1.05$ μm

The fiber design in Fig. 8(b) provides an example of a fiber with a much more extreme index contrast. The design target was to position the shortest ZDW at 1.05 μm to favor efficient supercontinuum generation in the near IR from an Yb fiber laser pump. The results in Fig. 7 indicate that a significantly large index contrast would be required for a lead silicate dispersion flattened SIF operating at around 1 μm . Simulations also showed that even for bismuth and tellurite core glasses a cladding with a refractive index typical of a liquid or a highly porous solid would be needed. In order to obtain an all solid fiber design we then explored the use of core glasses with even higher refractive indices. For example, the dispersion profile in Fig. 8(b), was obtained by fixing silica ($n = 1.450$) as the cladding material and a target dispersion $D_t = 0$ ps/nm/km at $\lambda_t = 1.05$ μm . It was found that a gallium lanthanum sulphide (GLS) based core glass ($n = 2.395$ at 1.05 μm) would provide sufficient waveguide dispersion to achieve the target, and that by setting $d = 0.68$ μm and $DS = 1.8$ ps/nm²/km the second ZDW could be positioned at sufficiently long wavelengths, around 1.5 μm . Interestingly, the combination of such a high index contrast with a sub- μm core, would produce a calculated effective nonlinearity of $220000 \text{ W}^{-1}\text{km}^{-1}$, suggesting that only millimeter to centimeter lengths would be sufficient for its application in nonlinear devices. The resulting nonlinearity and dispersion profile are promising properties for efficient supercontinuum generation from a fs/ps fiber laser pump [5]. We believe that fabrication of such a fiber could be possible either through the direct drawing of a silica capillary filled with a chalcogenide glass core or by high pressure pumping of the molten soft glass inside a silica hollow fiber.

6. Discussion and conclusions

We have investigated a novel approach to modify the waveguide dispersion and hence control the overall dispersive properties of highly nonlinear fibers. Rather than exploiting holes in the cladding, whose size and shape along the transverse and longitudinal direction is difficult to control in practice with the required level of accuracy, we propose using all-solid fibers with a large and suitably selected index difference between core and cladding. This solution results in a much simpler control of the structural properties of the fabricated fiber, which simplifies the practical achievement of any targeted dispersion profile. The obvious drawback of this method, as compared to holey fiber technology, is that for each fiber design a pair of glasses with specific index contrasts and compatible thermo-mechanical properties is required. However, as we have shown through the example of a fabricated fiber and through reference to results in the literature, a number of fabrication techniques are already available and could be further developed to fabricate such high Δn multi-glass fibers.

Through numerical simulations we have studied the dispersive properties of simple step-index fibers and shown how the overall dispersion and dispersion slope can be well controlled by adjusting core diameter and index contrast. Based on a few empirical rules, we have presented a general design method to obtain highly nonlinear fibers with tailored dispersive properties at a specific wavelength of interest, and an algorithm for the automatic design of dispersion controlled fibers. A few examples of realistically achievable fibers for telecoms all-optical processing and for supercontinuum generation have been also presented.

We have shown that the position of the ZMDW with respect to the operational wavelength is key to determining the structural parameters, the nonlinearity and ultimately the fabrication method of these dispersion controlled fibers. For operation at wavelengths much shorter than the ZMDW, high index contrasts and small core diameters are needed, producing extremely high nonlinearities. Operation at wavelengths longer the ZMDW reduces the effective nonlinearity of the fibers, due to larger cores and smaller index contrasts, but offers a wider dispersion controlled bandwidth. It is worth noting that in this latter operational regime fibers tend to satisfy the relation $(n_{co} - n_{cl})/n_{co} \ll 1$ and therefore can be effectively considered as 'weakly guiding'. As a results, their modes will be essentially linearly polarized (LP) and their properties can be predicted by using well known simplified methods [44,45].

We have also studied the singlemode condition for simple high contrast step index fibers and shown that single modality cannot be obtained when the waveguide dispersion contribution is anomalous. In this case an additional outer cladding forming a W-shaped profile may introduce a sufficiently large differential mode loss to generate effectively singlemode guidance even at wavelengths where the step-index equivalent fiber would be moderately multimode.

In conclusion, we believe that due to their outstanding nonlinear properties, combined with their highly tailorable and easily achievable dispersive properties, the all-solid, high index contrast fibers proposed in this work may play an important role in many future nonlinear optics based devices, from optical parametric oscillators and amplifiers to supercontinuum sources and all optical processing components.

Acknowledgments

This research has received funding from the Engineering and Physics Science Research Council (UK) and the European Communities Seventh Framework Programme FP/2007-2013 under grant agreement 224547 (PHASORS). Dr Francesco Poletti gratefully acknowledges the support of a Royal Society University Fellowship. The authors would like to thank Angela Camerlingo and Dr. Periklis Petropoulos for measuring the properties of the fabricated lead silicate W-profiled fiber.